supporting information accompanying:

Anion binding properties of a hollow Pd-cage

Brian J. J. Timmer[1] and Tiddo J. Mooibroek[1,*]

[1] van 't Hoff Institute for Molecular Sciences, Universiteit van Amsterdam, Science Park 904, 1098 XH Amsterdam, The Netherlands. *Corresponding author e-mail: t.j.mooibroek@uva.nl

Table of Contents

Attached seperately are .pdb files of Pd-complex **1** bound to NO_3^-, ClO_4^-, BF_4^- and PF_6^- that were geometry optimized with DFT at the ωB97X-D / 6-31G* level of theory.

Section S1. Materials and methods

All solvents and chemical were purchased from commercial suppliers and used without further purification. Compound **1** was prepared as previously described.[1] ^{1}H NMR titrations were performed using a Bruker DRX 500 spectrometer operating at 298 K. The residual solvent peaks were used as internal standards (^{1}H: δ 5.32 p.p.m., ^{13}C{^{1}H}: δ 53.84 p.p.m. for CD_2Cl_2; ^{1}H: δ 2.50 p.p.m., ^{13}C{^{1}H}: δ 39.52 p.p.m. for DMSO-d_6; ^{1}H: δ 1.94 p.p.m.), while ^{19}F NMR spectra were externally referenced to CF_3COOH (–76.55 p.p.m.). Chemical shifts (δ) are given in parts per million (p.p.m.).

The titrations were performed by stepwise addition of a solution of *n*-butyl ammonium salt to a solution of **1** (both in the same 9:1 DCM-d_2:DMSO-d_6 solution). Association constants (K_a) were determined by monitoring the change in chemical shift (Δδ) for a selected proton resonance of **1** and fitting these shifts to a 1:1 or 1:2 (host **1**: anionic guest) binding model using HypNMR.[2] An estimated goodness of fit was calculated as r^2 from all the observed and fitted Δδ values used in HypNMR.

Section S2. Titration Experiments

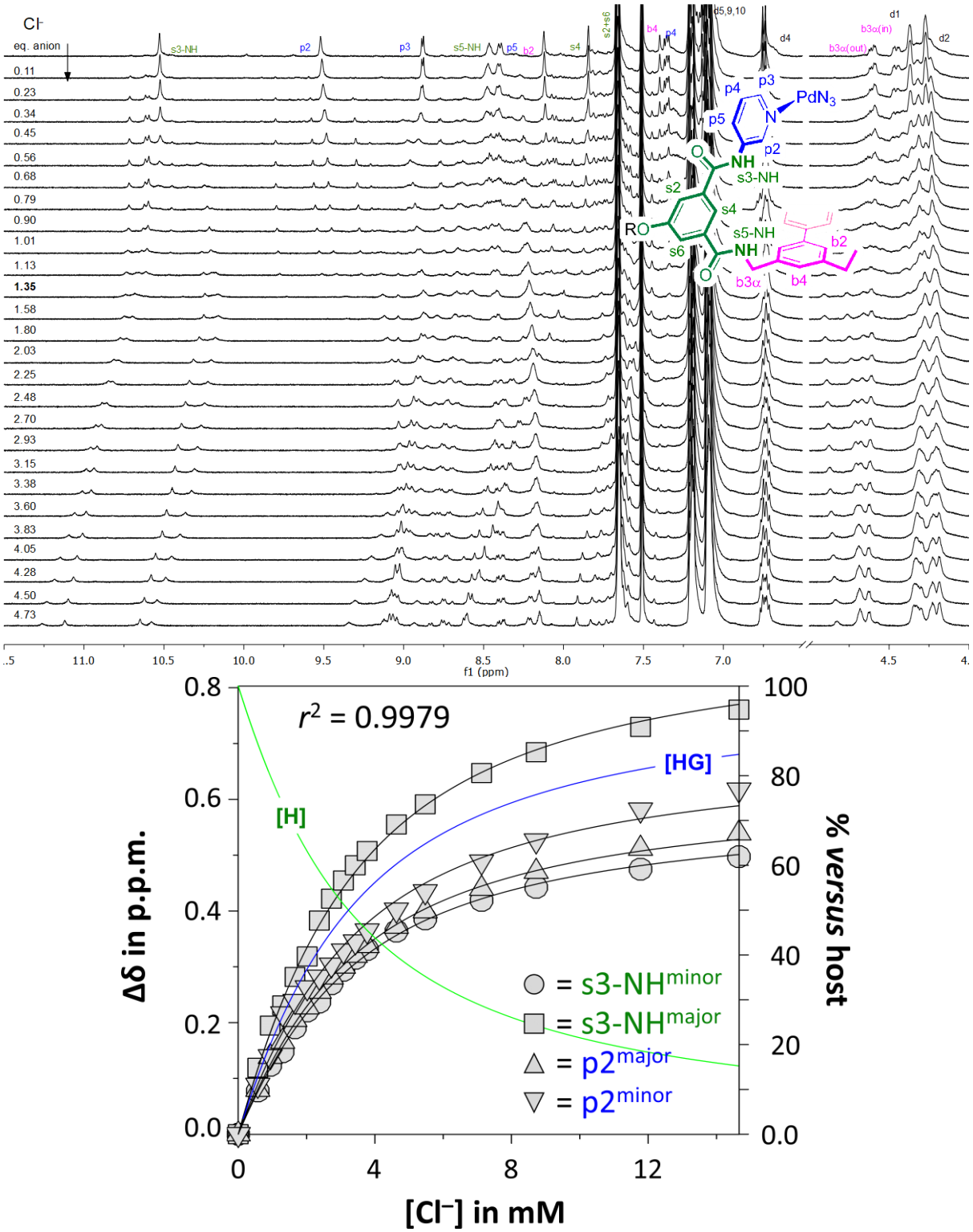

Figure S1. Top: ^{1}H NMR spectra and assignment of a binding study of 1.67 mM cage **1** with the *n*-butyl ammonium salt of Cl^{-} (112.6 mM) in CD_2Cl_2 with 10% DMSO-d_6. Bottom: HypNMR fit (speciation also given) on s3-NH and p2 of the major and minor species that became apparent after addition of about 1.3 equivalents of salt. K_a = 414 M^{-1} with indicated and goodness of fit (r^2). The fits are the lines through the symbols, which represent the data. Fitting the major and minor species separately gave nearly identical binding constants.

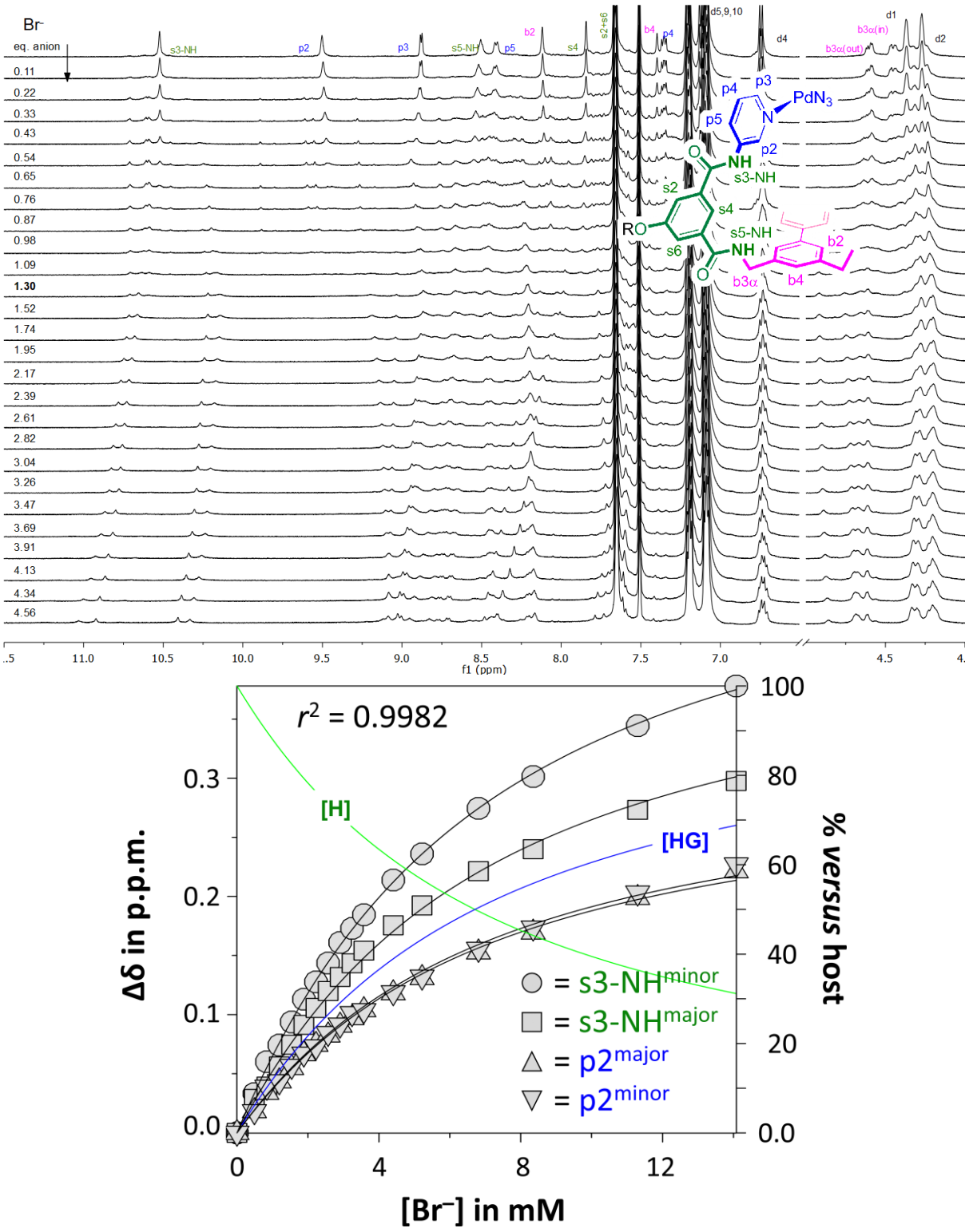

Figure S2. Top: ^{1}H NMR spectra and assignment of a binding study of 1.67 mM cage **1** with the *n*-butyl ammonium salt of Br^- (108.6 mM) in CD_2Cl_2 with 10% DMSO-d_6. Bottom: HypNMR fit (speciation also given) on s3-NH and p2 of the major and minor species that became apparent after addition of about 1.3 equivalents of salt. K_a = 169 M^{-1} with indicated and goodness of fit (r^2). The fits are the lines through the symbols, which represent the data. Fitting the major and minor species separately gave nearly identical binding constants.

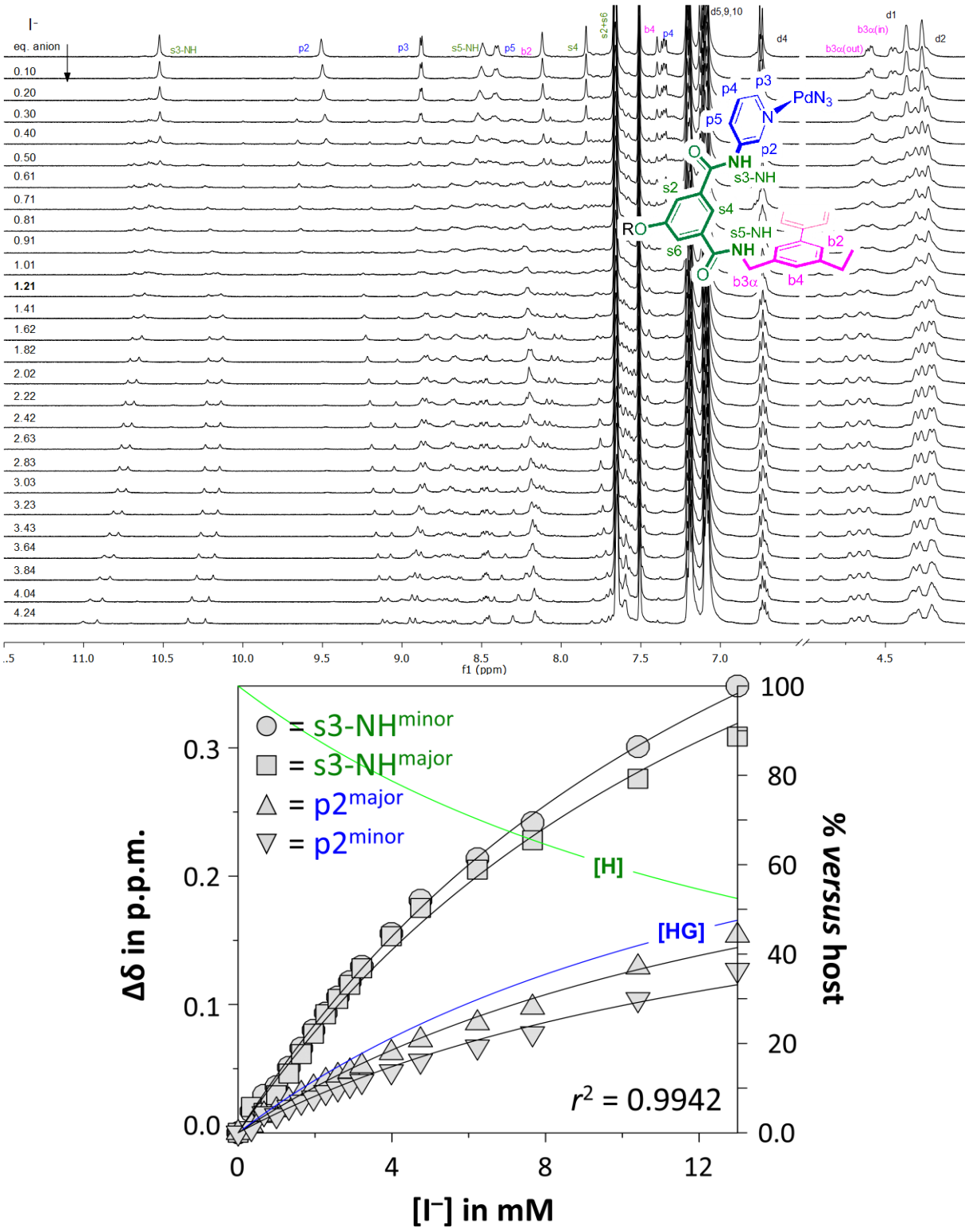

Figure S3. Top: ^{1}H NMR spectra and assignment of a binding study of 1.67 mM cage **1** with the *n*-butyl ammonium salt of I^- (101.0 mM) in CD_2Cl_2 with 10% DMSO-d_6. Bottom: HypNMR fit (speciation also given) on s3-NH and p2 of the major and minor species that became apparent after addition of about 1.2 equivalents of salt. K_a = 74 M^{-1} with indicated and goodness of fit (r^2). The fits are the lines through the symbols, which represent the data. Fitting the major and minor species separately gave nearly identical binding constants.

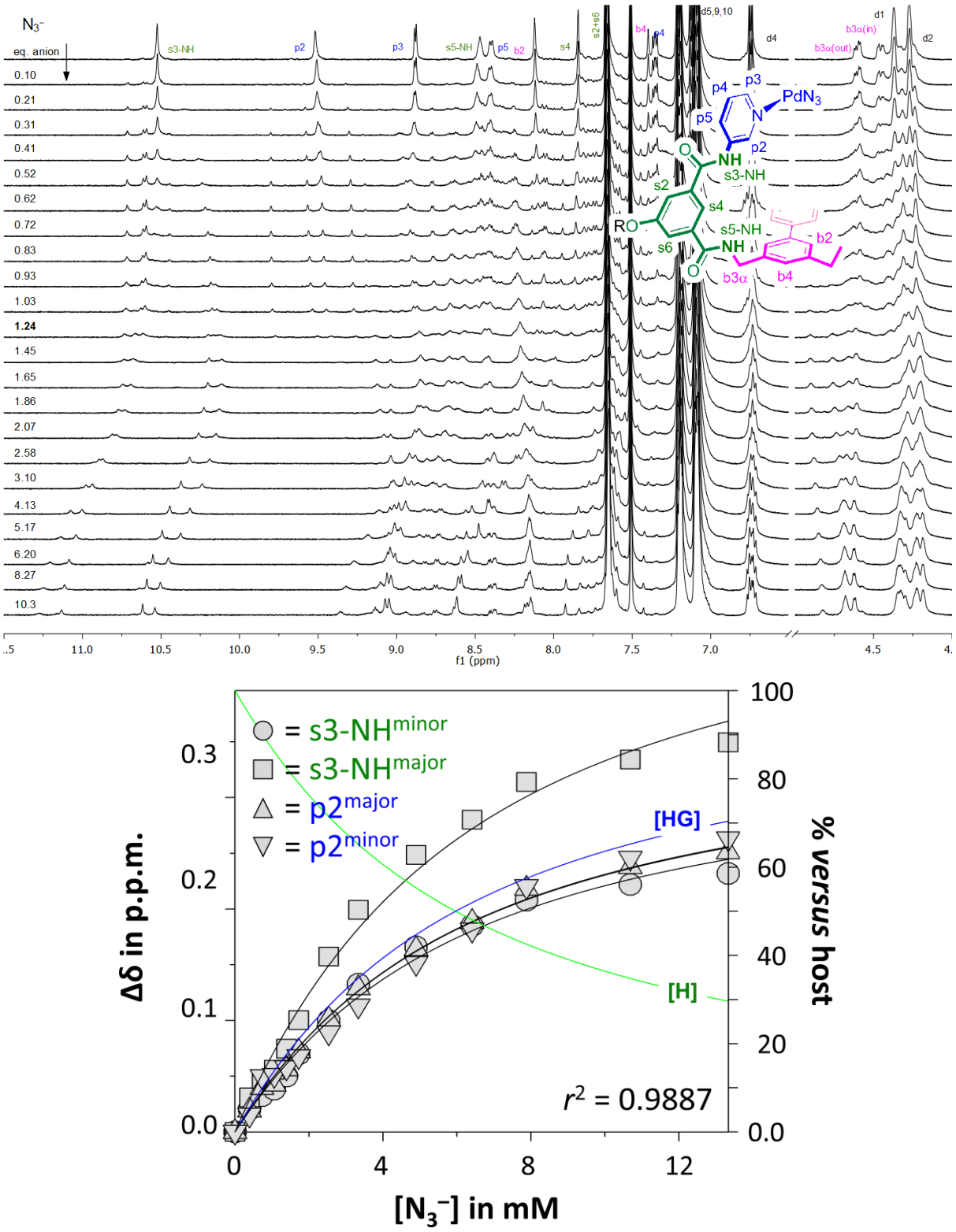

Figure S4. Top: ^{1}H NMR spectra and assignment of a binding study of 1.67 mM cage **1** with the *n*-butyl ammonium salt of N_3^- (103.3 mM) in CD_2Cl_2 with 10% DMSO-d_6. Bottom: HypNMR fit (speciation also given) on s3-NH and p2 of the major and minor species that became apparent after addition of about 1.2 equivalents of salt. K_a = 193 M^{-1} with indicated and goodness of fit (r^2). The fits are the lines through the symbols, which represent the data. Fitting the major and minor species separately gave nearly identical binding constants.

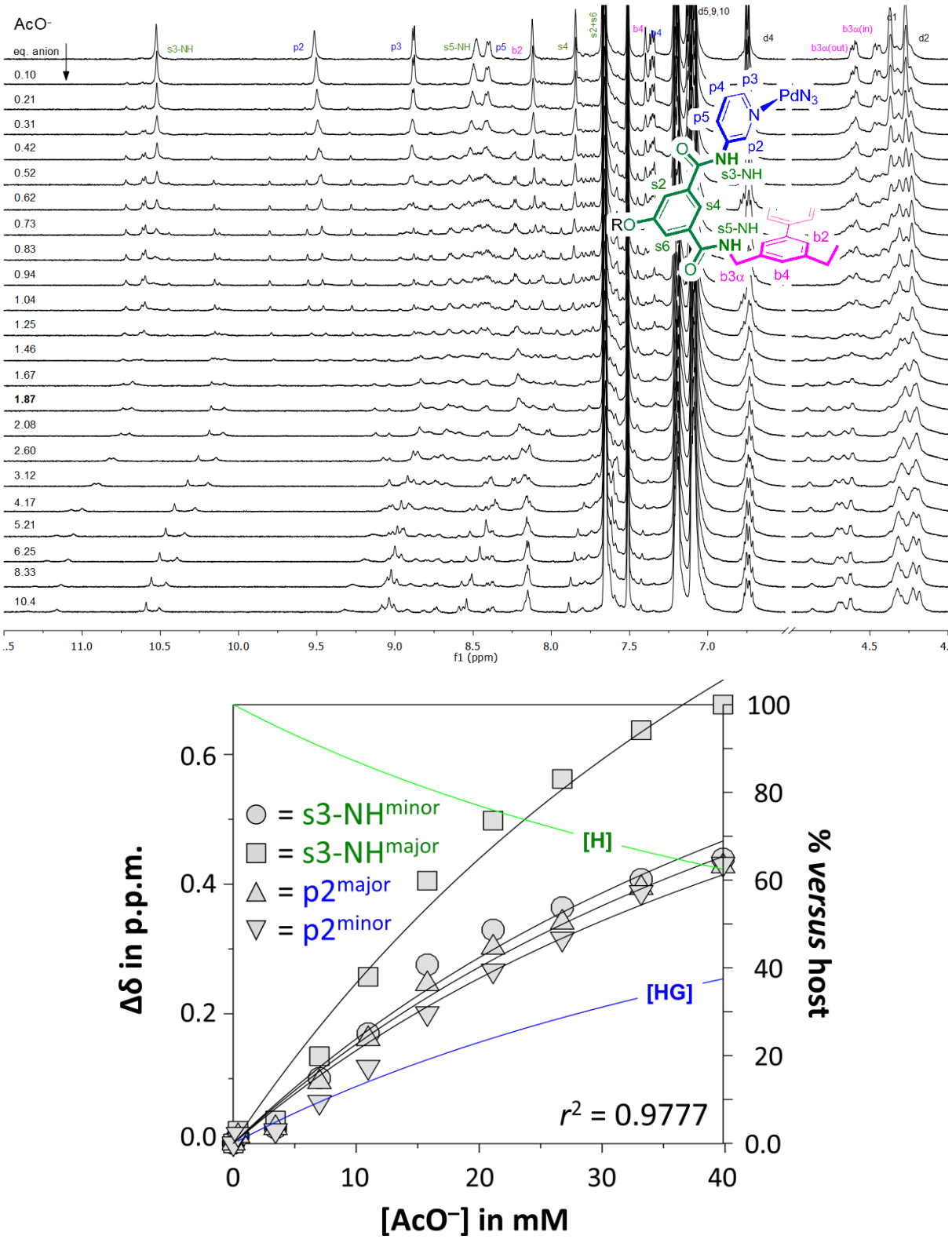

Figure S5. Top: ^{1}H NMR spectra and assignment of a binding study of 1.67 mM cage **1** with the *n*-butyl ammonium salt of AcO^- (104.1 mM) in CD_2Cl_2 with 10% DMSO-d_6. Bottom: HypNMR fit (speciation also given) on s3-NH and p2 of the major and minor species that became apparent after addition of about 1.9 equivalents of salt. K_a = 15 M^{-1} with indicated and goodness of fit (r^2). The fits are the lines through the symbols, which represent the data. Fitting the major and minor species separately gave nearly identical binding constants.

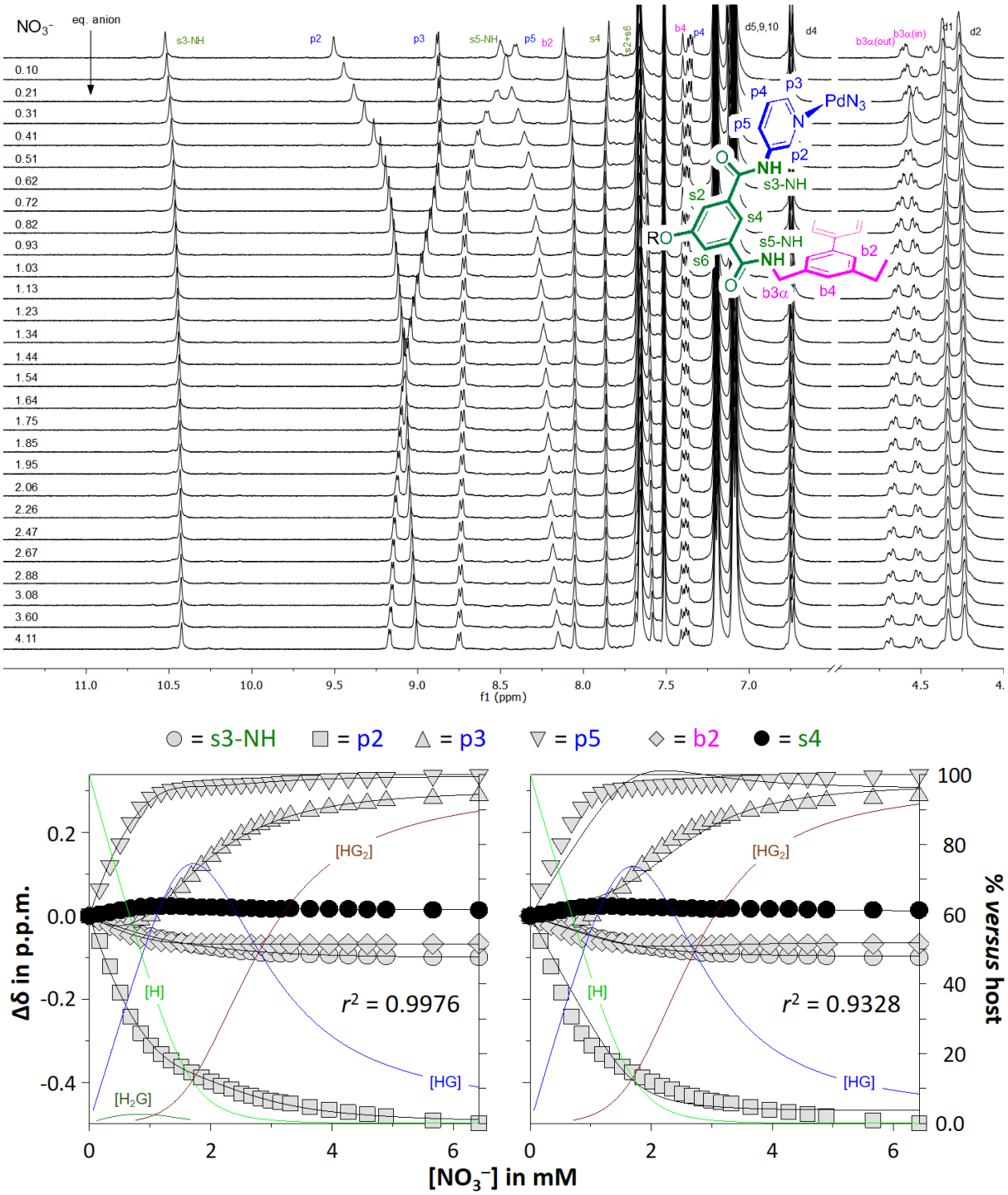

Figure S6. Top: ^{1}H NMR spectra and assignment of a binding study of 1.67 mM cage **1** with the *n*-butyl ammonium salt of NO_3^- (102.8 mM) in CD_2Cl_2 with 10% DMSO-d_6. Bottom: HypNMR fit (speciation also given) to a binding model using the indicated resonances. Fitting the date to a 1:1 model was not possible (HypNMR erred consistently). On the right is a 1:2 model, which fitted very poorly (r^2 = 0.9328 with $K_a^{1:1}$ = 100.000 M^{-1} and $K_a^{1:2}$ = 3162 M^{-1}) because apparent saturation occurred before the equivalents point (~1.7 mM). We affirmed that the concentrations of cage **1** was correct by integration on NMR after adding a known quantity of 1,3,5-triethylbenzene. Assuming an additional 2:1 binding ($K_a^{2:1}$ = 36 M^{-1}), where the nitrate anion bridges two cage molecules, gave the fit shown on the left-hand side. This fit was excellent (r^2 = 0.9976 over all 168 datapoints) and gave $K_a^{1:1}$ = 91.960 M^{-1} and $K_a^{1:2}$ = 2.484 M^{-1}). **NB:** the bridging capability of nitrate anions for $[Pd(pydidine)_4]^{2+}$ has also been observed in the solid state, as evidenced by structure FEDYOF shown in the main text in Figure 4.

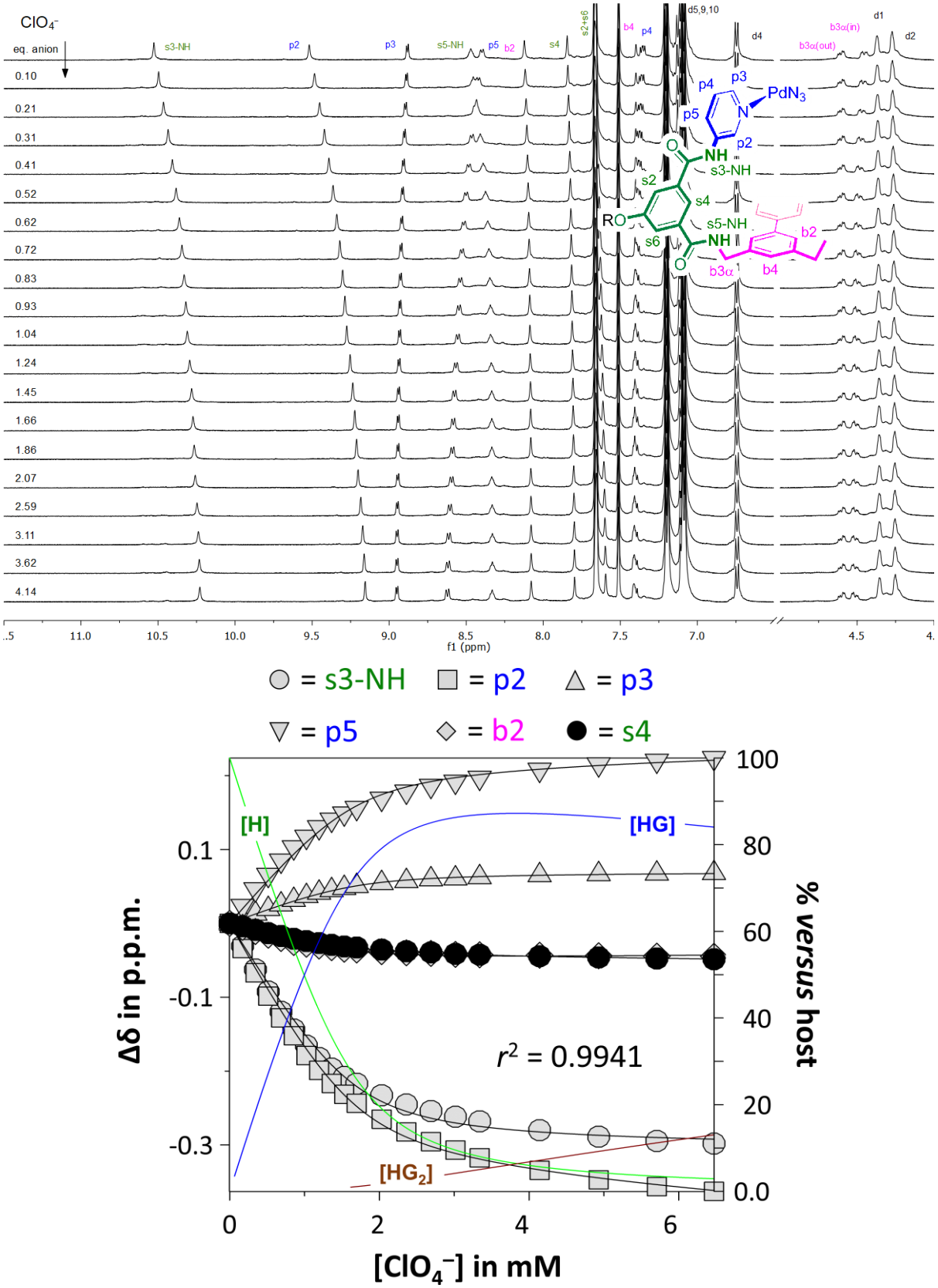

Figure S7. Top: ^{1}H NMR spectra and assignment of a binding study of 1.67 mM cage **1** with the *n*-butyl ammonium salt of ClO_4^- (103.5 mM) in CD_2Cl_2 with 10% DMSO-d_6. Bottom: HypNMR fit (speciation also given) to a 1:2 host:guest model using the indicated resonances. The fit gave $K_a^{1:1}$ = 6102 M^{-1} and $K_a^{1:2}$ = 33 M^{-1}, with indicated and goodness of fit (r^2) on all 120 datapoints. The fits are the lines through the symbols, which represent the data.

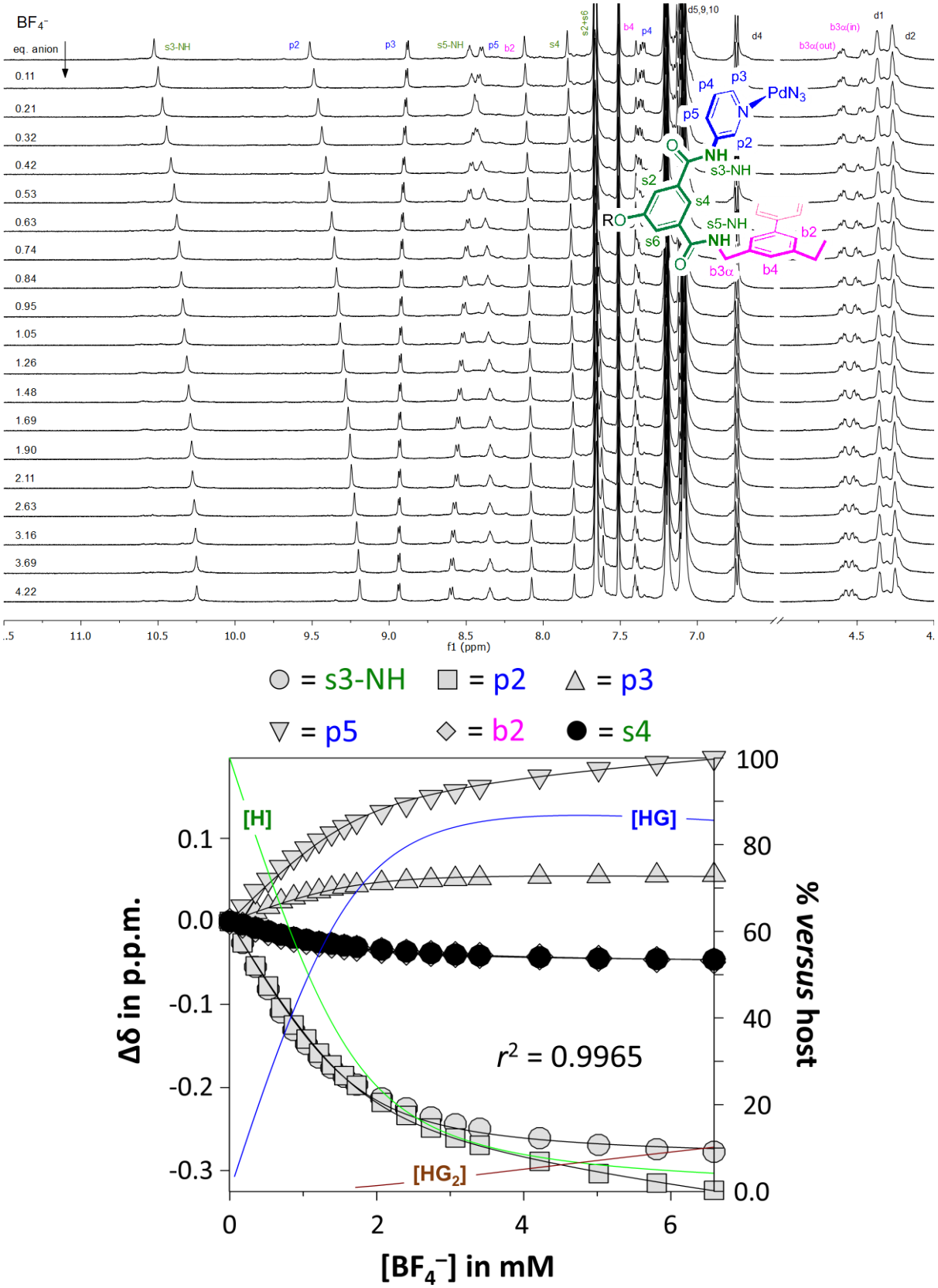

Figure S8. Top: ^{1}H NMR spectra and assignment of a binding study of 1.67 mM cage **1** with the *n*-butyl ammonium salt of BF_4^- (105.4 mM) in CD_2Cl_2 with 10% DMSO-d_6. Bottom: HypNMR fit (speciation also given) to a 1:2 host:guest model using the indicated resonances. The fit gave $K_a^{1:1}$ = 4141 M^{-1} and $K_a^{1:2}$ = 24 M^{-1}, with indicated and goodness of fit (r^2) on all 120 datapoints. The fits are the lines through the symbols, which represent the data.

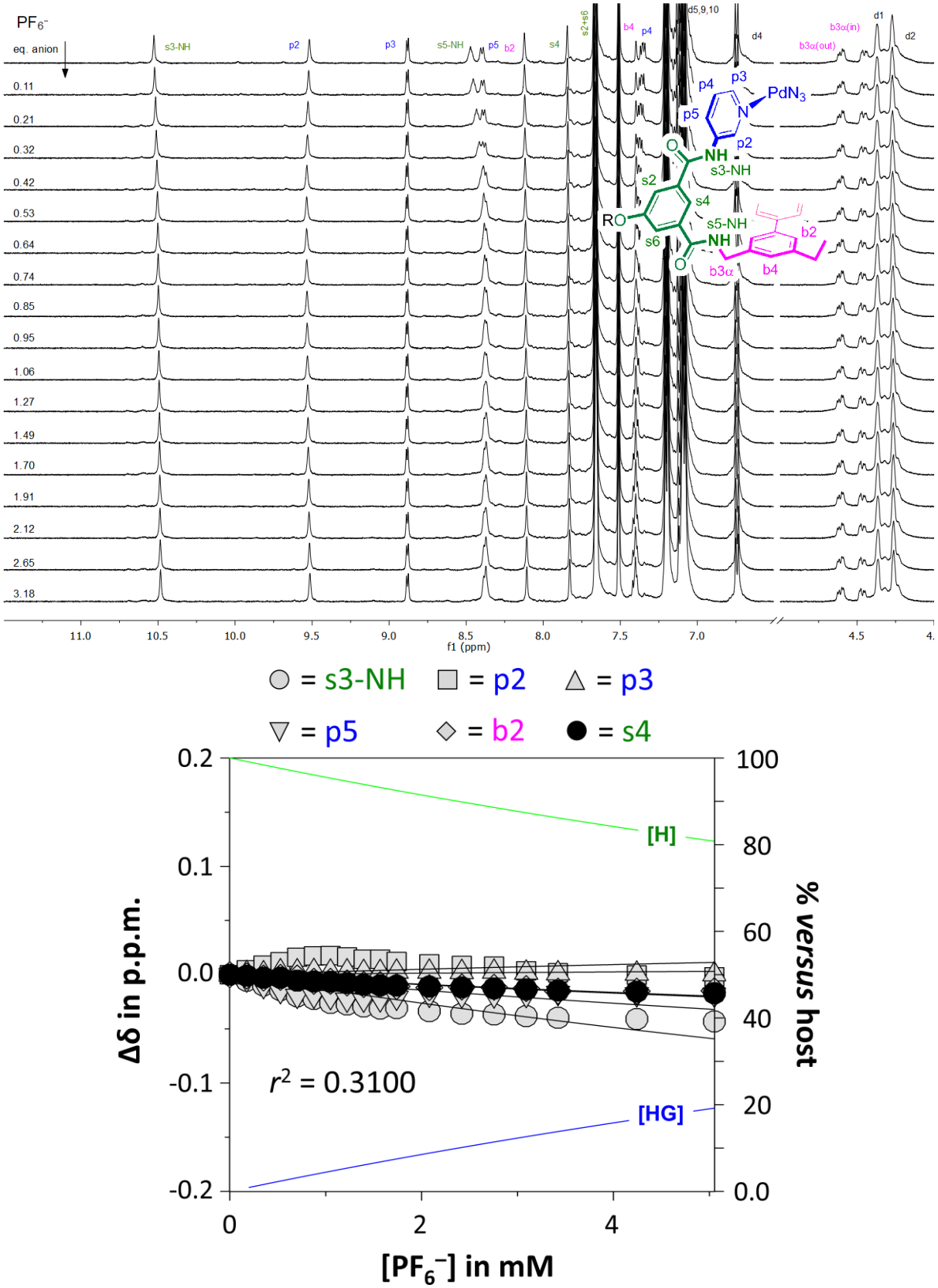

Figure S9. Top: ^{1}H NMR spectra and assignment of a binding study of 1.67 mM cage **1** with the *n*-butyl ammonium salt of PF_6^- (106.1 mM) in CD_2Cl_2 with 10% DMSO-d_6. Bottom: HypNMR 1:1 host:guest model using to model the indicated resonances (speciation also given). The model assumed a K_a of 50 M^{-1} giving a very poor indicated goodness of fit (r^2) on all 120 data points. Adjusting the binding constant or assuming a 1:2 model did not improve the fit. Given the very small shifts observed relative to the titrations with ClO_4^- and BF_4^-, it is likely that PF_6^- does not bind at all (or has a very low affinity, near the detection limit under the conditions used).

Section S3. {^{1}H-^{19}F}-HOESY NMR

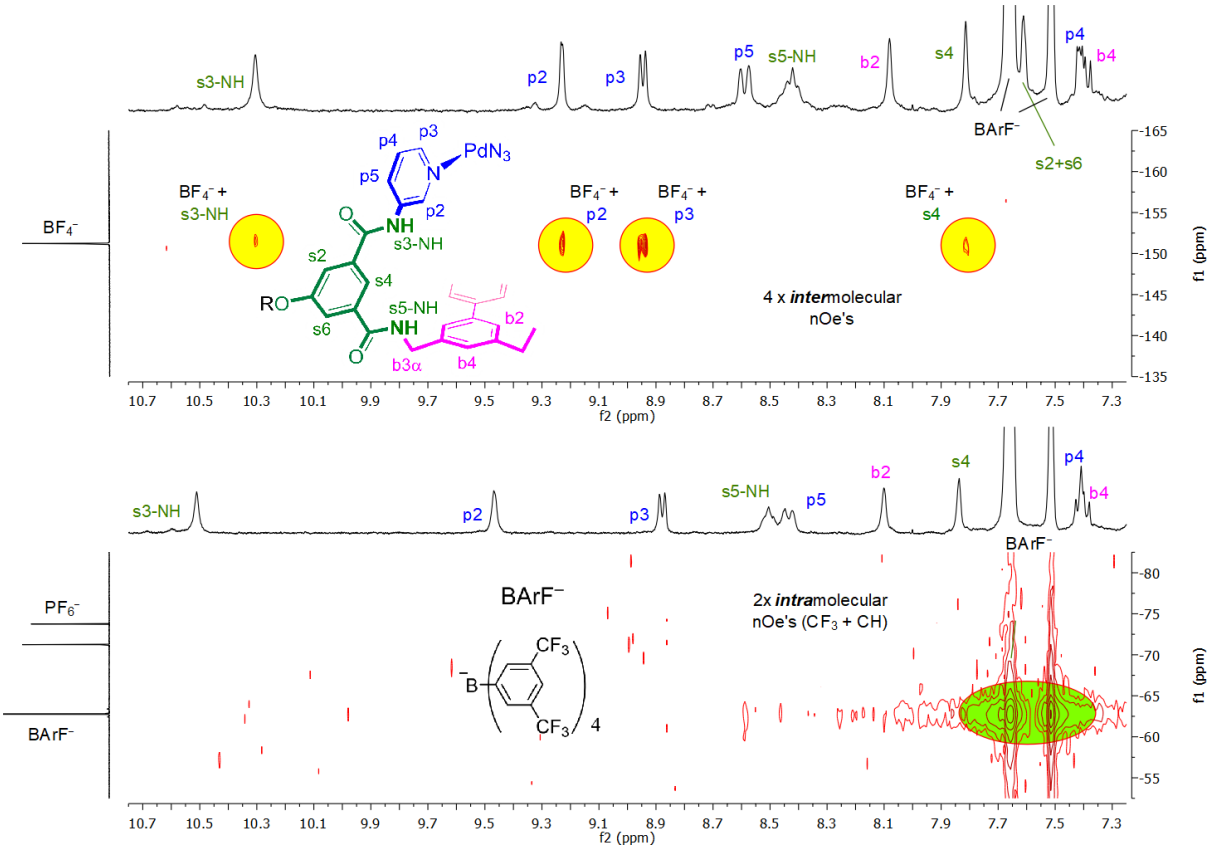

Figure S10. {^{1}H-^{19}F} HOESY NMR spectra of the titration of **1** with BF_4^- (top) and PF_6^- (bottom) at concentrations similar to those obtained at the end of the titration experiments (see Figure S8 and Figure S9 respectively). For the sample containing BF_4^-, there are four clear intermolecular nOe's (highlighted in yellow). Three of these involve the inwards pointing **s3-NH**, **p2** and **s4**, thus evidencing the binding mode to the interior of **1**. An additional nOe involves the outwards pointing **p3**, evidencing an additional binding mode with the exterior of **1**. For the sample containing PF_6^-, there only are the intramolecular nOe signals expected for the BAr^F anions (green highlight) while no intermolecular nOe's with resonances of **1** were detected.

Section S4. Model of $[1 \bullet PF_6]^+$

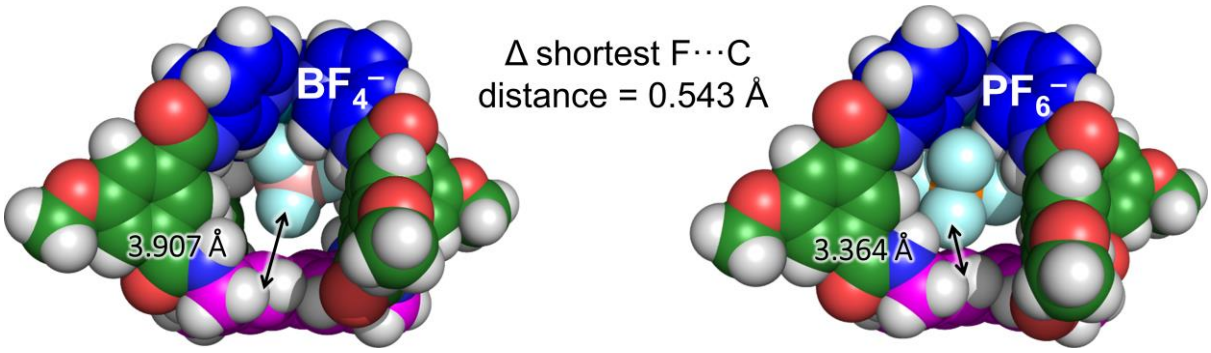

Figure S11. Comparison of the molecular models of **1** with interior bound BF_4^- (left) and PF_6^- (right) computed in the gas phase with DFT at the ωB97X-D / 6-31G* level of theory. The shortest measured F···C distance in each adducts is given. This distance of 3.364 Å in the PF_6^- adduct is 0.543 Å shorter than in the BF_4^- adduct. Actually, the distance of 3.364 Å is close to the sum of the van der Waals radii of F (1.47) and C (1.70), i.e. 3.17 Å and thus suggests that PF_6^- barely fits the cavity of **1** in this model. These distances can thus help to rationalize the observed absence of binding with PF_6^- (i.e.: repulsion between the negative F and the negative π-cloud of the biphenyl). The larger size of PF_6^- also means that the negative charge is spread out over a larger area so that PF_6^- will be 'softer' and thus engage in weaker hydrogen bonding interactions.

Section S5. CSD survey

The Cambridge Structure Database version 5.41 including three updates until August 2020 was inspected with ConQuest version 2020.2.0 (Build 290188). A Pd complex with four pyridyl (NC_5) ligands was drawn where one C-atoms *ortho* to the pyridyl N had a H attached and the substitution of the other C-atoms was left unspecified. The Pd–N bonds as well as the N–O bonds were specified as 'any'. The anion was drawn as well and the query was run to obtain the amount of CSD entries containing both the anion and the Pd(pyridyl)$_4$ complex (N^{total}).

In another query, one C–H···O/F(anion) distance was set as intermolecular interactions with van der Waals overlap using the van der Waals radii implemented in ConQuest (i.e.: 1.20 Å for H, 1.52 Å for O and 1.47 Å for F). This query was run to obtain the amount of CSD entries where at least one C–H···O/F(anion) bonding interaction was present (N^{vdW}).

In the CSD entries where a H···O/F(anion) bonding interaction was found, there were typically multiple such interactions. The sum total of all these interactions found was also gather ($N^{vdw\text{-}total}$), together with the average van der Waals corrected distances (i.e.: d^{vdW} = H···O/F distance – the van der Waals radii of the elements involved).

Given in Table 1 is a numerical overview of the searches, showing that hydrogen bonding interactions with ortho-H's of Pd-pyridyl like complexes with anions are rather common in the solid state. Moreover, the average amount of van der Waals overlap (between 0.15 and 0.23 Å) is substantial. What also stands out is that the average van der Waals overlap is ordered NO_3^- > ClO_4^- ≈ BF_4^- >> PF_6^-. This exact order is also observed in the average number of C–H···anion bonding interactions found per CSD entry (i.e. $N^{vdW\text{-}total}$ / N^{vdW}). Both these observations are consistent with the order of binding constants obtained from titration experiments.

Table S1. Overview of CIFs that contain a Pd(Pyridyl)$_4$-like complex where at least one *ortho* C–H is in close contact with the O/F of the indicated anion.

Anion	N^{total}	N^{vdW}	$N^{vdW\text{-}total}$	d^{vdW}
NO_3^-	122	82 (67%)[a]	556 (6.8x)[b]	-0.227 ± 0.131 Å
ClO_4^-	14	11 (79%)[a]	61 (5.5x)[b]	-0.201 ± 0.135 Å
BF_4^-	117	85 (73%)[a]	465 (5.5x)[b]	-0.216 ± 0.128 Å
PF_6^-	45	35 (78%)[a]	117 (3.3x)[b]	-0.149 ± 0.102 Å

[a] percentage relative to N^{total}; [b] average number of C–H···O/F(anion) bonding interactions per CSD entry (i.e. $N^{vdW\text{-}total}$ / N^{vdW}).

References

[1] *Angewandte Chemie International Edition*, 2021, *DOI:10.1002/anie.202104924*
[2] *Analytical Biochemistry*, 1995, *231*, 374–382.